David Cunningham W7BEP
Doppler Systems
111 E. Moon Valley Drive
Phoenix AZ 85022

DF Breakthrough!

— the "turkey" tracker we've all been waiting for

A U.S. Patent is pending on the direction-finding system described in this article. For further information, contact the author.

Radio direction-finding (RDF) systems tend to fall into two general categories depending on whether or not they use the Doppler shift principle. Most non-Doppler RDFs employ directional antennas which produce peaks or nulls in the received signal amplitude as they are rotated. Doppler-type systems, on the other hand, detect the phase modulation imparted to the received signal by translational motion of the receiving antenna. As a consequence of the "capture effect" of the FM receiver which detects the phase modulation, Doppler-type systems generally are less sensitive to site errors than amplitude measurement systems. The first known RDF based on detecting the Doppler shift was patented by H.T. Budenbom and used a motor driven antenna. Doppler RDFs today do not mechanically rotate an antenna, but instead rely on sequential switching between a series of antennas placed in a circular array to approximate the continuously rotating single element.

In 1969, W7KWB and I built one of the earliest adaptations of this system for amateur use. That system employed 16 switched antennas housed in a 4-foot-diameter wooden "hat box" and was used successfully in local transmitter hunts during 1970-1972. The antenna itself was heavy (115 pounds) and the system required an external oscilloscope for display. DTL logic was used. Other systems were subsequently built in the Phoenix area which operated on essentially the same basis but incorporated improved mechanical construction and utilized the more sophisticated TTL and CMOS integrated circuits then becoming available.

A serious drawback to these systems was the drastic loss in sensitivity which occurred during operation. A second problem which was equally vexing was the appearance of mysterious false bearing vectors apparently due to off-channel frequencies being shifted onto the received frequency by something in the commutation (electrical rotation) process. Both of the above problems would disappear whenever the antenna commutation was halted, i.e., on-channel stations would immediately regain their signal strength into the receiver and off-channel carriers would disappear.

Several techniques were tried unsuccessfully to eliminate these problems. Theorizing that the switching transients related to turning on and off the various antennas were causing receiver desensitization and, in addition, were modulating off-channel signals into the receiver passband, several methods were investigated to smooth out the switching transients. These included:

(1) overlapping the antenna selection so that at least

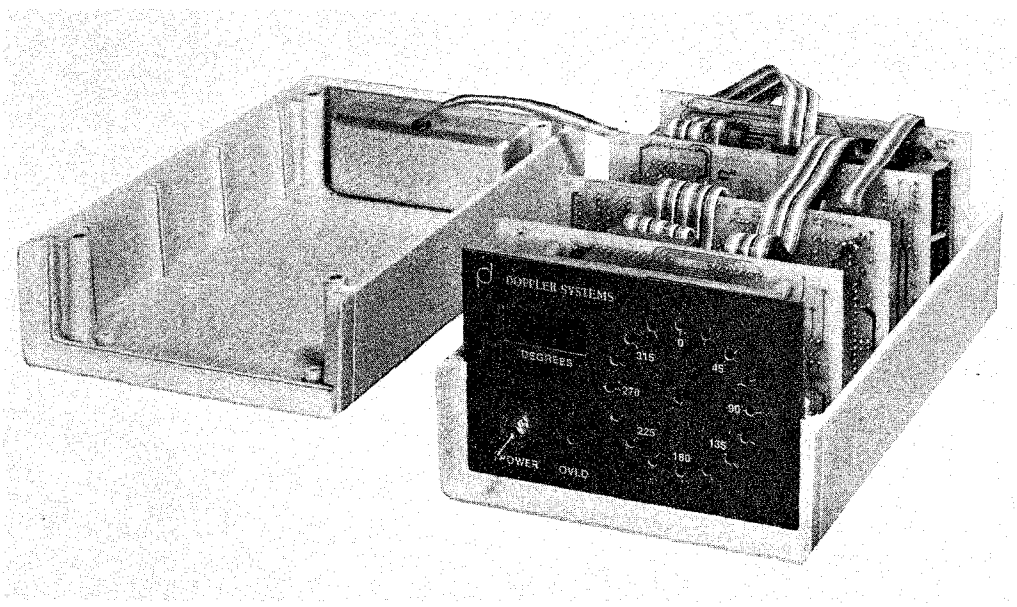

Photo A. Fully expanded version of the electronics available in kit form from Doppler Systems.

one antenna was always connected to the receiver;

(2) rounding the antenna switching waveforms and using PIN diodes to create a more gradual on/off transition; and

(3) generating a complex analog control waveform matched to the gain characteristics of the PIN diodes to further reduce switching transients.

None of these solutions produced especially noteworthy results. In addition, it was felt that an antenna array of the size being used was impractical, especially for mobile use. Reducing the number of elements would help this problem, but with discrete commutation, the linearity of the system deteriorates as the number of antennas decreases.

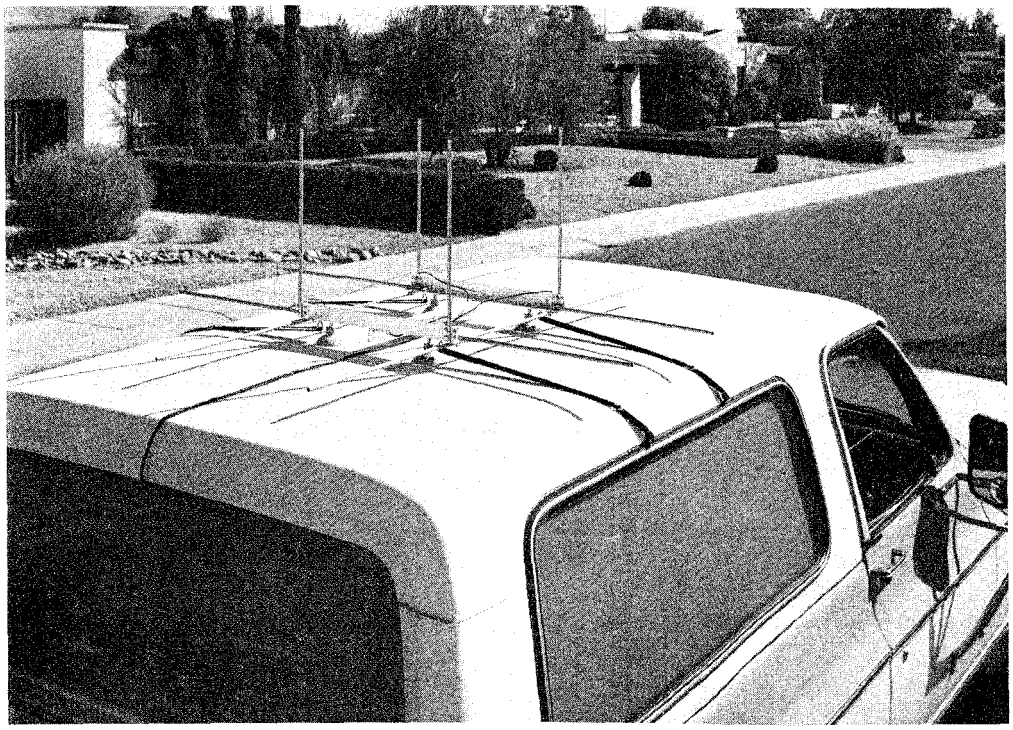

Photo B. Antenna mounted to a 1974 Blazer. The ground plane formed by the radials is particularly useful with non-metallic roofs.

The solution which ultimately was discovered uses only four antennas which are located in a square pattern, the sides of which are typically 1/4 wavelength long. The received signal induced into all four antennas is continuously mixed in a precision summing circuit in such a manner that the resultant rf voltage produced is very nearly identical to that which would be induced in a single antenna rotating at a uniform rate around the circle which inscribes the square formed by the four actual antennas. Tests have demonstrated that this system does not possess the loss of gain or off-channel susceptibility problems of previous designs. Antenna size for VHF applications is very compact. Electronic processing is relatively involved, but considering the performance which is obtained, it is justified for serious direction-finding applications. The system to be described works with any FM receiver to detect the Doppler-induced phase modulation and does not require any modification of the receiver. It is relatively broadband and has been tested over the frequency range of 135 to 165 MHz.

Depending on the application, three different outputs are available. For mobile application, a circular array of 16 light-emitting diodes (LEDs) provides an immediate analog bearing relative to the vehicle's direction. For more demanding mobile or fixed station applications, a 3-digit panel display provides the bearing directly in degrees. Finally, a serial interface is available in a format suitable for remote-display (utilizing the same or similar electronics for readout), recording the bearing data on an ordinary audio tape recorder, or connection to a microprocessor. The linking of several remotely-located direction finders into a common microprocessor for automatic station triangulation and logging should be straightforward.

A simplified functional block diagram of the complete system is shown in Fig. 1. The rf summer combines the output of the four antennas in a manner which phase-modulates the rf signal to the receiver. As explained on the next section, the phase modulation contains the bearing information. A conventional FM receiver provides the audio input to the Doppler signal processor via connection to the external speaker output. Synchronous filtering removes the normal voice content leaving a sine wave having the same frequency as was used to modulate the antenna signals and a phase angle equal to the bearing angle. This sine wave acts as a trigger to latch the outputs of counters for display of the bearing in either a circular LED array and/or a 3-digit decimal display. An optional serial interface transmits the bearing data displayed by the unit or receives external bearing data as input for the display.

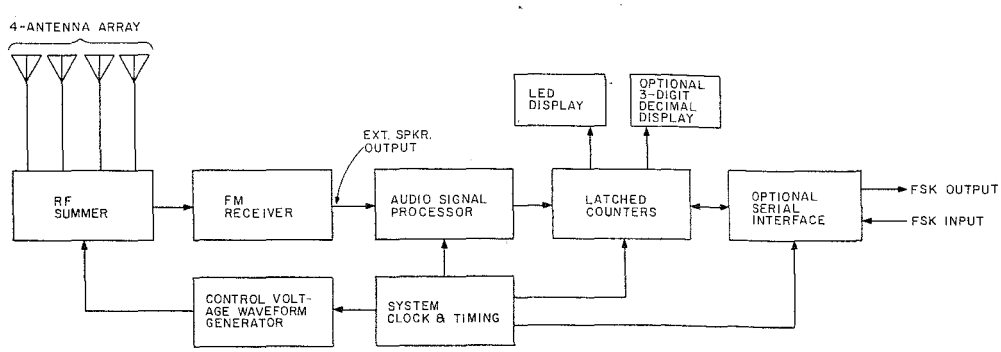

Fig. 1. Block diagram of the complete direction-finding system.

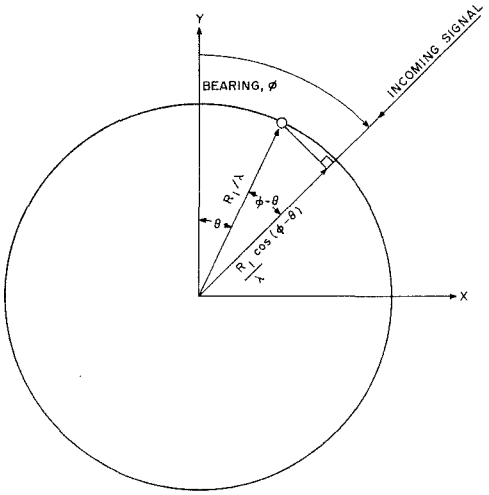

Fig. 2. Geometry used to derive the signal received by a rotating antenna.

Theory

Fig. 2 illustrates a simple antenna located at distance R_1/λ and angle θ from the reference position. Assume the incoming signal is located far (relative to the wavelength, λ) from the receiving antenna at the bearing ϕ shown. Then the voltage induced in the antenna can be written as shown in Equation (1), where A is the received amplitude in volts, ω_c is the carrier frequency in radians per second, t is the time in seconds and is selected to start with a zero crossing of E_R at the origin, and ψ is the phase shift in radians due to the antenna being closer to or further from the transmitter. If the antenna is closer to the source, ψ would be positive, indicating a phase lead, etc. For the geometry shown, see Equation (2).

Now suppose the receiving antenna is permitted to rotate with velocity ω_d in a circular path of radius R_1/λ. Then $\theta = \omega_d t$ and the phase of the received signal is as shown in Equation (3).

Equation (3) indicates that the rotating antenna has caused the incoming carrier to become phase (and frequency) modulated. The modulation frequency is the same as the rotation frequency, ω_d, so the frequency deviation which is equal to the rate of change of the phase is as shown in Equation (4) or Equation (5).

A standard FM receiver with de-emphasis will produce an audio output equal to the phase which is modulating the received signal (assuming the deviation is small compared to the discriminator full-scale range). See Equation (6).

Thus the receiver's audio output is a sinusoid having a frequency equal to the antenna commutation frequency, ω_d, and a phase angle equal to the bearing angle, ϕ. The commutation frequency should be selected to be at the low end of the receiver's audio passband to facilitate filtering out the normal voice modulation of the received signal.

Another way of looking at the problem is to consider the situation when the rotating antenna is at the angle where it is directly approaching the incoming signal. The maximum relative velocity causes an apparent increase in the carrier frequency at this point. Similarly, when the antenna has moved 180 degrees to the point where it is traveling away from the transmitter, the relative velocity is a minimum and the carrier frequency appears to be lower. This is the familiar Doppler shift phenomenon, but here the rotation of the antenna produces a periodic up/down shift, the phase of which is set by the bearing angle between receiver and transmitter.

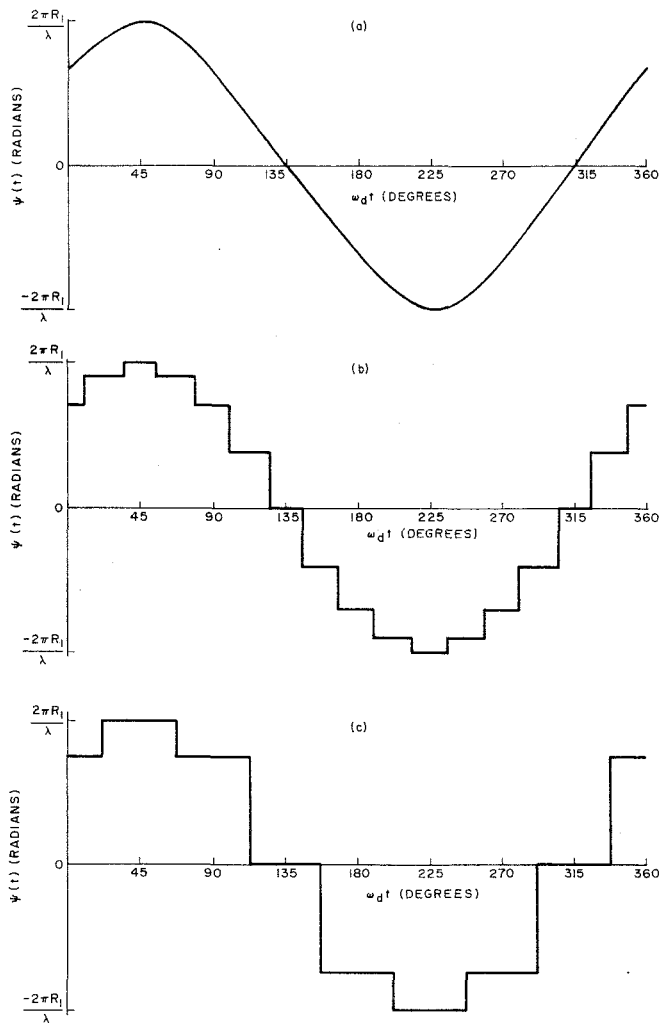

Fig. 3. Waveforms illustrating the phase modulation imparted to the received signal when the bearing angle is 45 degrees.

Fig. 3(a) shows Equation (3) plotted against time for an assumed bearing angle of 45 degrees. Instead of physically rotating a single antenna, present-day Doppler systems discretely switch between adjacent antennas located in a circular array. To indicate graphically what sort of waveforms are generated by discretely commutated antenna arrays, the theoretical audio output for a system of 16 and 8 antennas is plotted in Figs. 3(b) and 3(c), respectively. The antenna, of course, receives many different signals in addition to the channel of interest. The phase modulation of all of these signals by a complex waveform such as shown in Fig. 3(b) or 3(c) may generate a variety of frequency components within the receiver passband. It is believed that these spurious frequencies are responsible for the false bearing problems noted earlier.

The technique for electronically producing the phase modulation of Fig. 3(a) with four antennas will now be described. Consider the system of antennas A, B, C, and D shown in Fig. 4 and assume for the moment

that the antennas are not coupled; i.e., there is no mutual impedance between them. The signals received by the four antennas can be summed electronically as shown in Equation (7), where K_A, K_B, K_C, K_D are gains and E_A, E_B, E_C, E_D are the rf voltages induced in the four antennas. We wish to find the value of the four gains which will create a voltage E_S equal to that induced in an antenna S located on the inscribed circle of radius R_1/λ at the angle θ shown in Fig. 4.

If an incoming signal were arriving from the left or right in Fig. 4, the phase at A and B would be equal, and the phase at C and D would also be equal. As long as the array is less than 1/2 wavelength on a side, the phase at point S may be computed by interpolating linearly between the phases to the left and right as indicated in the plot directly below the sketch of the antenna array in Fig. 4. See Equation (8).

For example, if S is midway between A and D, $\theta = 0°$, $K_X = 1/2$, $(1-K_X) = 1/2$, and the phase is the simple average of the phases measured at A and D. If we now consider a signal originating from the top in Fig. 4, the phase at S can be computed from that at A or D and that at B or C by interpolating along the Y direction. Referring to the graph to the left of the antenna in Fig. 4 see Equation (9).

Equations (8) and (9) may be combined to give a two dimensional interpolation of phase. From similarity, Equation (7) can then be written as in Equation (10).

The mixing is not perfect since rf voltages rather than phase angles are being mixed; the errors, however, are small, as discussed below. The gain for antenna A is given in Equation (11), which is shown plotted in Fig. 5 over one cycle of rotation in θ. Note that the gain peaks, as would be expected, at 45 degrees where the imaginary antenna is closest to antenna A. A second small gain increase also occurs 180 degrees from this location. The other antenna gains, K_B, K_C, and K_D, have identical shapes to K_A, but are displaced 90 degrees in phase (K_B lags K_A by 90°, etc.).

To evaluate the accuracy of the mixing given by (10), the instantaneous amplitude and phase of E_S was computed for antennas of different size with various bearing angles, ϕ. A typical result is shown in Fig. 6 for an antenna of dimension $2R_1/\lambda = 1/4$ on each side. In

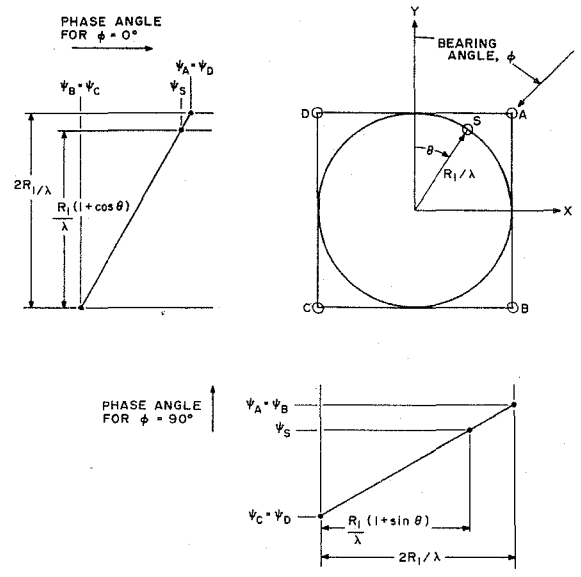

Fig. 4. Top view of a four-antenna array showing the interpolation of phase angle between opposite sides of the array.

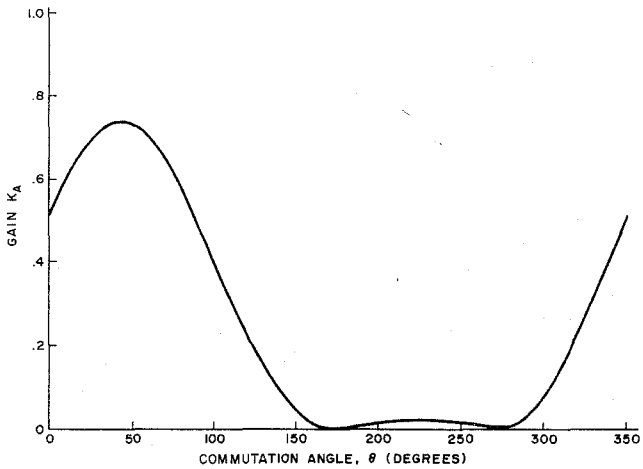

Fig. 5. Theoretical gain variation for antenna "A" required to produce an equivalent continuously rotating antenna signal.

EQUATIONS

Equation (1): $E_R = A \sin(\omega_C t + \Psi)$

Equation (2): $\Psi = \frac{2\pi R_1}{\lambda} \cos(\phi - \theta)$

Equation (3): $\Psi(t) = \frac{2\pi R_1}{\lambda} \cos(\phi - \omega_d t)$

Equation (4): $\omega_{deviation} = \frac{2\pi R_1 \omega_d}{\lambda}$ radians/second

Equation (5): $f_{deviation} = \frac{R_1 \omega_d}{\lambda}$ Hz

Equation (6): $E_{audio} = K_A \frac{2\pi R_1}{\lambda} \cos(\phi - \omega_d t)$

Equation (7): $E_S = K_A E_A + K_B E_B + K_C E_C + K_D E_D$

Equation (8): Phase at $S = \Psi_S = \Psi_{C \text{ or } D} + \left[\frac{(1 + \sin\theta) R_1/\lambda}{2 R_1/\lambda}\right] (\Psi_{A \text{ or } B} - \Psi_{C \text{ or } D})$

$= K_X \Psi_{A \text{ or } B} + (1 - K_X) \Psi_{C \text{ or } D}$

where $K_X = (1 + \sin\theta)/2$

Equation (9): $\Psi_S = \Psi_{B \text{ or } C} + \left[\frac{(1 + \cos\theta) R_1/\lambda}{2R_1/\lambda}\right] (\Psi_{A \text{ or } D} - \Psi_{B \text{ or } C})$

$= K_Y \Psi_{A \text{ or } D} + (1 - K_Y) \Psi_{B \text{ or } C}$

where $K_Y = (1 + \cos\theta)/2$

Equation (10): $E_S = K_X K_Y E_A + K_X(1 - K_Y) E_B + (1 - K_X)(1 - K_Y) E_C + (1 - K_X) K_Y E_D$

Equation (11): $K_A = K_X K_Y = 1/4 (1 + \sin\theta)(1 + \cos\theta)$

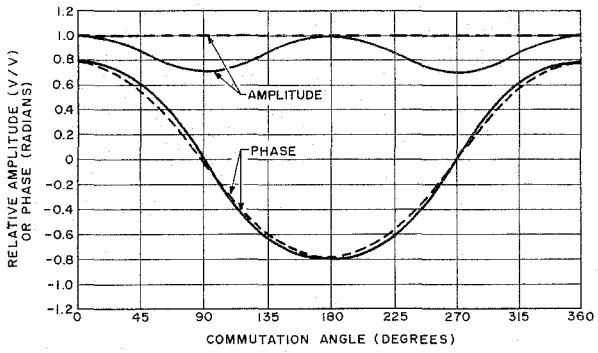

Fig. 6. Amplitude and phase modulation for an uncoupled antenna array of size 1/4 wavelength and a bearing angle of 0 degrees. The dashed lines represent the ideal (continuously rotating antenna) case.

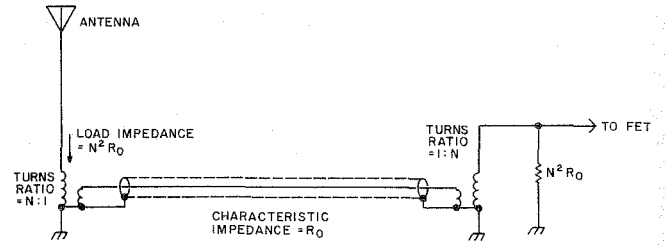

Fig. 7. Use of impedance transformers to minimize the effect of mutual impedance coupling between array antennas.

Fig. 6, the bearing angle ϕ is 0 (signal coming from top in Fig. 4). The composite rf signal contains some amplitude modulation (about 18% at twice the commutation frequency) in addition to the desired phase modulation. Note that the phase modulation error relative to an ideal (physically rotating) antenna is very small (less than 8%).

At bearing angles of 22.5 and 45.0 degrees, the amplitude modulation is lower and the phase modulation error is about the same—better than 8%. Antenna symmetry causes the amplitude and phase error characteristic to repeat every 45 degrees of bearing. Decreasing the antenna size improves the error characteristic over that shown in Fig. 6, but antenna tolerances become more critical and the magnitude of the phase modulation (deviation) which must be detected decreases as given by Equation (5).

The above results were based on an antenna array in which the elements do not interact with each other—that is, a current flowing in one antenna element does not induce a voltage in one of the other elements. This is generally not the case for antennas spaced at these distances.

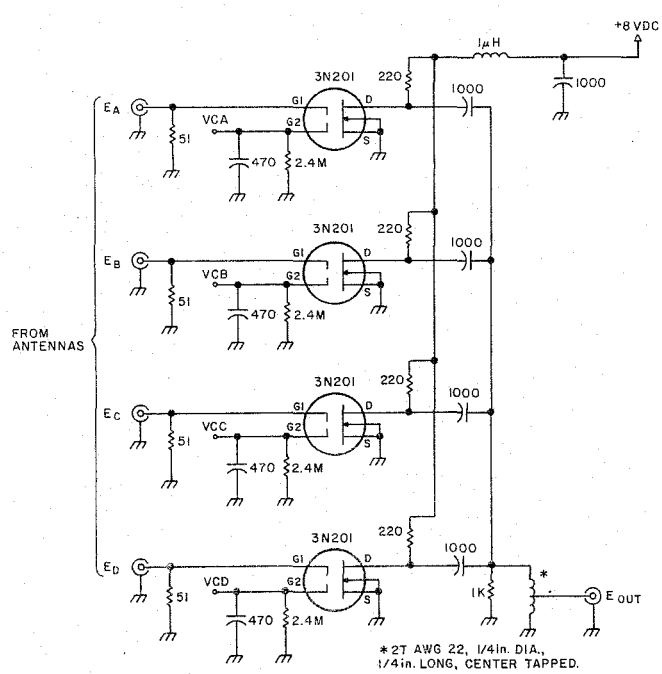

Fig. 8. Rf summer circuit schematic.

A detailed analysis has been made which takes into account the actual coupling between elements (mutual impedance). If each antenna element is terminated into a 50-Ohm load, the antenna currents and hence the coupling between elements are significant and the rf output voltage to the receiver is affected. For the 1/4-wavelength array, amplitude modulation increases to about 65% and the phase modulation waveform becomes noticeably distorted. The situation is considerably better with smaller antennas. For example, if the array size is 1/8 wavelength on a side, the amplitude modulation is only 19% and the phase modulation is very nearly sinusoidal.

An alternate to reducing the array size is to increase the effective load impedance across each antenna element. This may be accomplished using an impedance step-down transformer at the antenna and an impedance step-up transformer at the receiving end of the transmission line. See Fig. 7. It should be kept in mind that in a receiving application, the antenna is acting as the source and the receiver (or rf summer here) is the load. We wish to minimize standing waves on the transmission line to prevent rf pickup other than from the antenna. Therefore, the line must be matched to the rf summer. At the antenna, we are interested in having the maximum voltage developed across the antenna terminals. This is obviously obtained by presenting a high impedance load to the antenna. An impedance match between line and antenna is generally regarded as essential to proper system operation, but that is the case only for transmitting where the antenna acting as the load determines the line swr and maximum power transfer occurs when line and load are matched.

At this point, it might be asked just how significant amplitude modulation and phase modulation distortion are in this system. The receiver provides limiting which will remove most of the AM, and the phase detector provides synchronous filtering which will remove most of the harmonic distortion in the phase modulation. Initially, it was feared that any amplitude modulation would cause modulation products from adjacent channel signals to be formed which might appear on the selected channel and cause interference. Also, distortion of the phase modulation could lead to bearing errors at specific bearing angles. Neither of these problems has been observed in either the testing or the field use of this system. Therefore, while a solution is at hand, the need to employ it has not been evidenced and the design to be discussed in the remainder of this article does not include impedance transformers. The subject

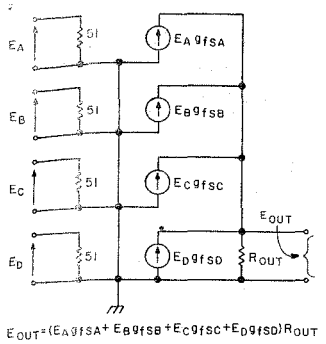

Fig. 9. Equivalent circuit of the rf summer.

of antenna array optimization and coupling for this system is an area for much additional experimentation and development.

Rf Summer

The circuit to be used for antenna summing should provide a low insertion loss, provide a stable and electronically-controlled gain characteristic, have negligible phase-shift variation with the control voltage, be compatible with a 50-Ohm unbalanced input, and lend itself to operating into a 50-Ohm unbalanced output.

PIN diodes and voltage-controlled FET resistor devices were tried and eventually rejected for one or more incompatibilities with the above requirements. The dual-gate MOSFET operating in a common-source configuration was found to provide an excellent choice. Fig. 8 shows the circuit configuration.

The rf equivalent circuit is given in Fig. 9. Each MOSFET acts as a current source into a common output impedance. The single, tapped inductor is used to cancel the combined output susceptance of the four MOSFETs. Device input impedance is extremely high, and the circuit is broadbanded by the use of relatively low value resistors for line impedance termination at all inputs and the output. Some gain is lost, but it is quite acceptable (less than 6 dB) and could easily be made up with a preamplifier stage at the output if desired. The output voltage is the weighted sum of the four antenna voltages with the weighting determined by the transconductance of the FETs. Since the transconductance can be varied by the second gate control voltage, this provides the means for electronically combining the rf voltages.

Fig. 10 plots the measured circuit gain (E_{out}/E_{in}) of four randomly selected devices together with a 7th order polynomial fit to the data. By combining the MOSFET rf gain characteristic of Fig. 10 with the desired antenna gain variation given in Fig. 5, the control voltage waveform for antenna A can be found. This is plotted in Fig. 11. The control waveforms for channels B, C, and D are identical in shape, but delayed by 90, 180, and 270 degrees respectively.

Control Voltage Waveform Generator

Two inexpensive PROMs are used to store the waveform plotted in Fig. 11. The PROM address is multiplexed in multiples of 90 degrees commutation angle, and the PROM output, after conversion to an analog voltage, is demultiplexed at the same time so that the entire PROM memory is utilized to generate each of the four control voltages. Fig. 12 shows the schematic of the control voltage waveform generator.

The CD4040 is a 12-stage ripple-carry binary counter that produces an 8-bit incrementing address to the PROMs. When driven at a frequency of 1,228,800 Hz, the PROM address will cycle at a rate of 300 Hz, which is the commutation frequency of the system. To multiplex the PROM, the two most significant bits

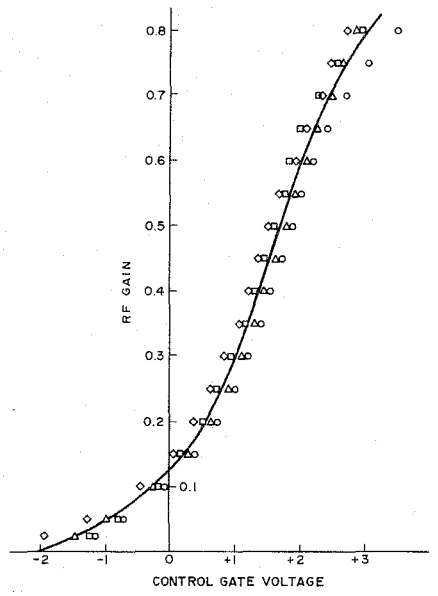

Fig. 10. Rf gain variation with control gate voltage for four typical field-effect transistors. The curve is a seventh-order polynomial fit to the measured data.

are modified by adding a 0, 1, 2, and 3 sequentially to each of the PROM addresses using a CD4008 full adder. The resulting address is held temporarily in the 8-bit 74LS273 latch which synchronizes the otherwise skewed output of the ripple counter.

Together, the two 74S287 PROMs provide an 8-bit address by 8-bit output memory for the control waveform. Each address corresponds to 360/256 or 1.40625 degress of commutation, while the output is scaled to cover the range −2.5 to +3.5 volts dc which provides a resolution of 6.0/256 = 0.0234 volts/step. The MC1408 digital-to-analog converter is used with a CA3240 BIMOS operational amplifier to minimize offset and noise. The CD4051 is an 8-channel analog demultiplexer which directs the converter output into one of the four dual-gate MOSFETs. A small RC filter formed by the 10-kilohm resistors and 470-pF capacitors in the rf summer is sufficient to hold the demultiplexed control voltage between updates. NAND gates A and B are used to inhibit the demultiplexer except during that portion of the cycle when the D/A output is stable. They also provide the synchronizing pulse to the 74LS273 octal latch.

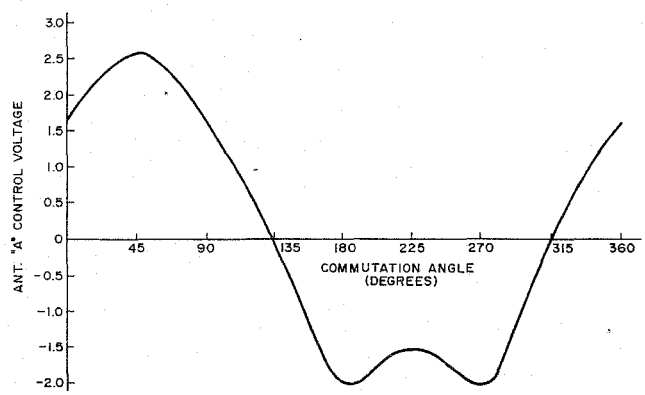

Fig. 11. FET control voltage required to produce the amplitude variation shown in Fig. 5.

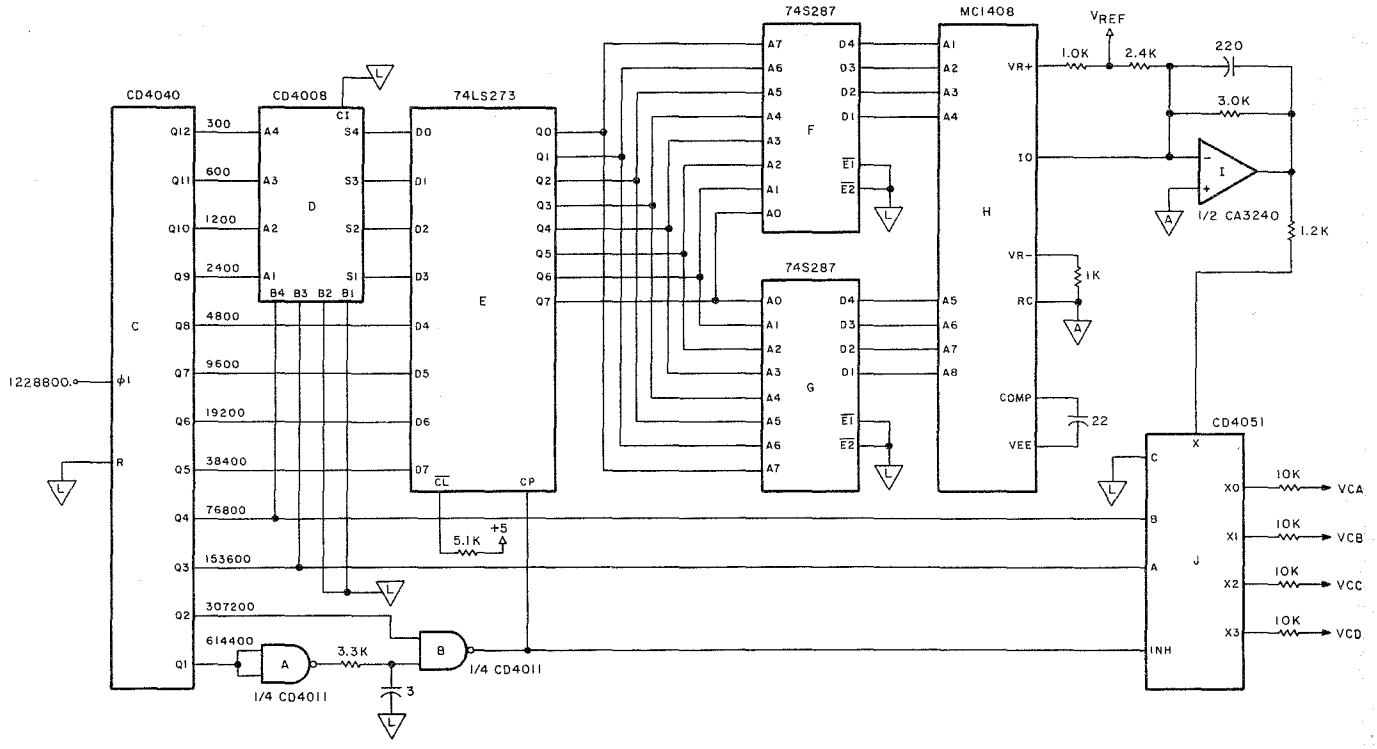

Fig. 12. Circuit schematic of the control voltage waveform generator. Notes: Logic power is Vcc = Vdd = +5, Vee = −6, Vss = GND = ⏚. Op amp power is +5 and −6 V dc.

Audio Signal Processor

Fig. 13 shows the circuitry used to extract the 300-Hz Doppler modulation frequency from the receiver's audio output and generate a logic signal synchronized to the phase of this signal for the display generator. Threshold detectors are also provided to give an overload indication to assist in setting up the audio gain of the circuit and to blank the display when no signal is present.

Preamplifier A is ac coupled to the receiver and contains a gain adjustment variable over the range 0.2 to 10. Frequencies below 142 Hz are attenuated by the input filter and frequencies above 664 Hz are reduced by the feedback compensation. Amplifier B provides an additional gain

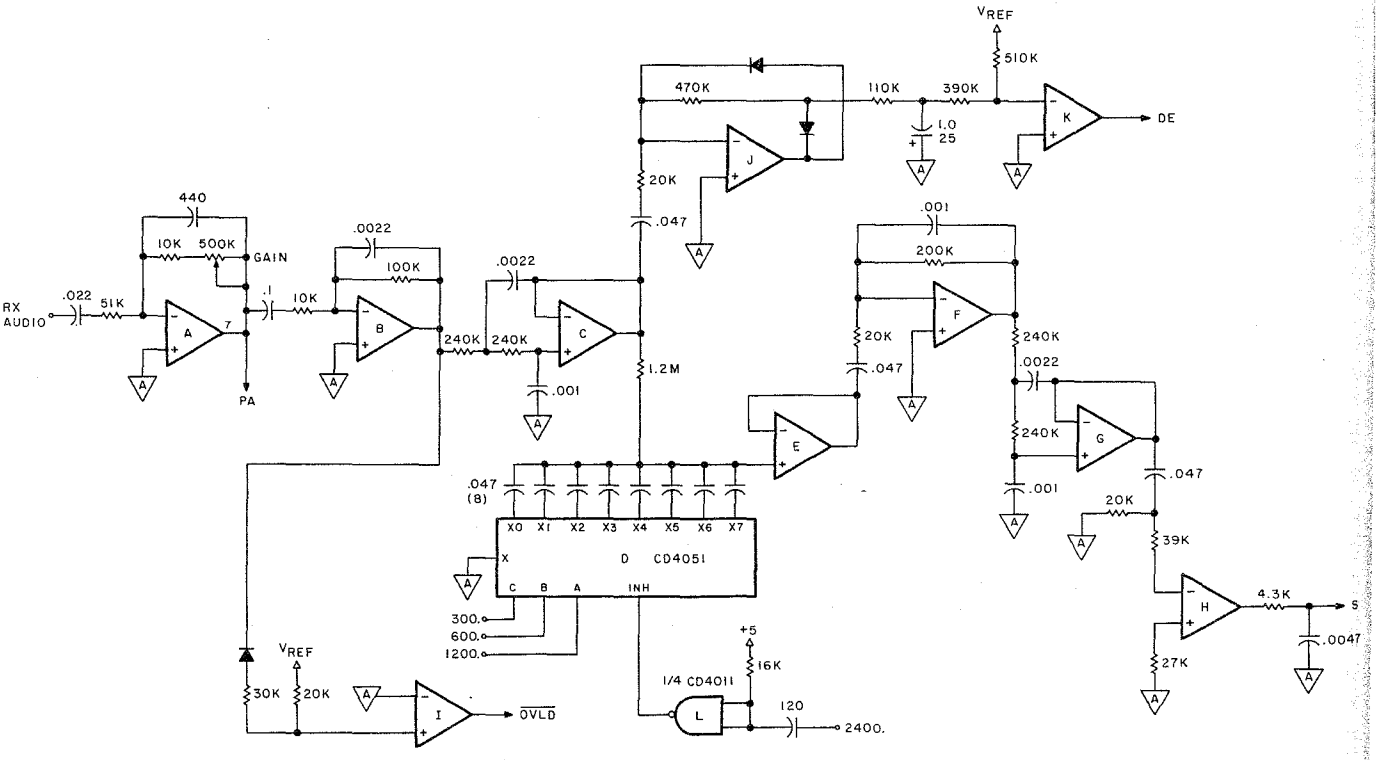

Fig. 13. Audio signal processor circuit schematic. Notes: All op amps are 1/2 LM1458 except H, which is 1/2 CA3240. All diodes are 1N4148. Logic power is Vdd = +5, Vee = −6, Vss = ⏚. Op amp power is +5 and −6 V dc.

of 10 and further filtering above 724 Hz.

Amplifiers C and G are identical second-order lowpass filters tuned to a frequency of 469 Hz with critical damping. These filters and the commutative filter described below were designed using the methods given in "Get Notch Qs in the Hundreds," by Mike Kaufman, *Electronic Design* 16, August 2, 1974, pp. 96-101.

The 8-section commutative filter, composed of multiplexer D and follower amplifier E, provides a 300-Hz bandpass synchronized to the antenna waveform frequency with a Q of 7540 RC where R is the series input resistor and C is the value of each of the switched capacitors. In Fig. 13, R = 1.2 megohms and C = .047 uF, providing a Q of 425. Since the Q of this circuit determines the speed of response of the system as well as the selectivity, a trade-off can be made in the selection of resistor R. The value shown provides a good compromise, but individual users may prefer a somewhat faster or slower responding display. The one-shot formed with NAND gate L is used to inhibit switching of the multiplexer during transition of its logic-select inputs.

Amplifier F provides an additional gain of 10 and helps to attenuate harmonics produced in the commutative filter above 796 Hz. Ac coupling is used to attenuate frequencies below 169 Hz because the commutative filter does pass dc. Amplifier H is used as a comparator to produce a square wave sync signal for the display generator. A CA3240 operational amplifier is used here instead of the LM1458s used elsewhere for its very high slew rate. Ac coupling is employed to remove any dc offsets from the previous two stages, and a small RC filter at the output prevents extremely short sync pulses from being generated with zero input.

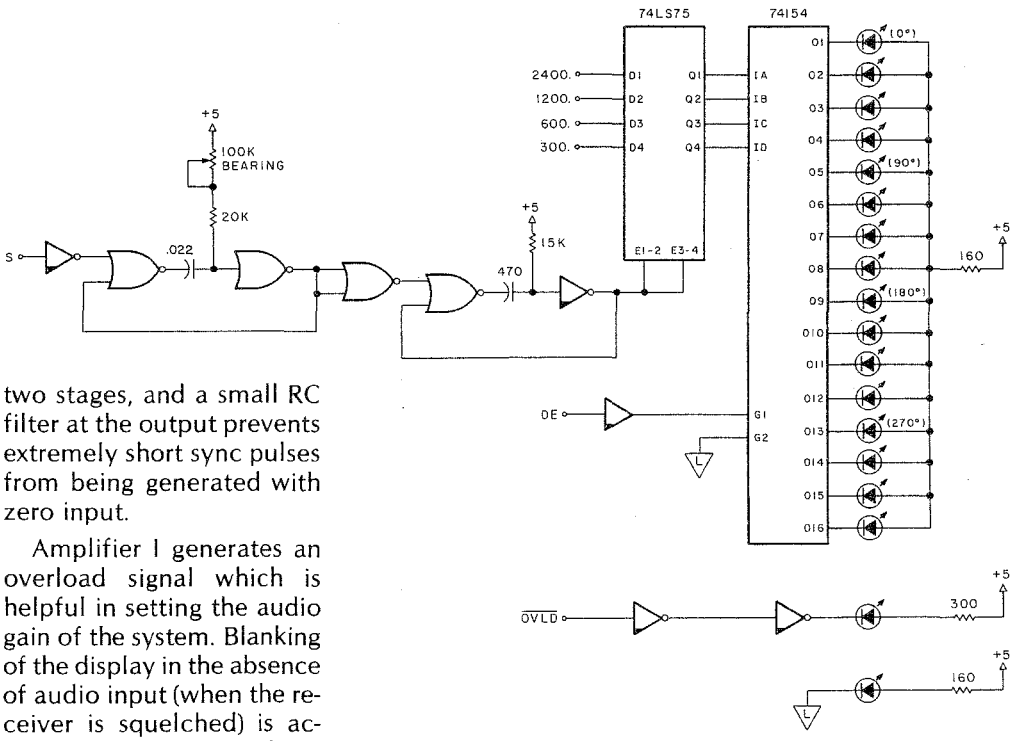

Fig. 14. Simple LED display circuit schematic. Notes: All LEDs are MIL32 R. Logic power is Vcc = Vdd = +5, Vss = GND = L NOR gates are 1/4 CD4001. Inverters are 1/6 74C903.

Amplifier I generates an overload signal which is helpful in setting the audio gain of the system. Blanking of the display in the absence of audio input (when the receiver is squelched) is accomplished by the half-wave rectification of amplifier J and the comparator operation of amplifier K. A blanking delay of approximately 100 milliseconds is provided by the electrolytic capacitor.

Display

The circuitry required for a simple LED display is shown in Fig. 14. Two one-shot circuits are used to convert square wave sync signal S to a short positive clock pulse which is used to latch the binary clock count into the 74LS75 quad latch. The first one-shot has an adjustable delay time to permit calibration of the display over a 90-degree bearing angle. (Rotation of the four antenna inputs is used for greater correction.) The second one-shot generates the 10-microsecond latching pulse.

A 74154 decoder drives the 16-LED circular display directly. Two additional LEDs are used to indicate audio overload in the signal processing circuit and the power-on status.

When both LED and three-digit decimal bearing readouts are required, the circuit of Fig. 15 is used in place of Fig. 14. This circuit is designed for compatibility with the optional serial interface to be described below and uses a 4-bit data bus to transfer data between temporary holding registers and the display latches. If the serial interface is omitted, the two signals $\overline{\text{SEND}}$ and MS must be tied to logic ground.

BCD counter latches H, I, and J are driven by a 108,026-Hz clock signal and their contents are latched into tri-state latches O, P, and Q by the delayed sync pulse. The binary clock count is simultaneously strobed into latch R by the same sync pulse. Since the maximum count is (decimal) 359, the maximum BCD count required for the hundreds digit is 3 (binary 0011). Since the two most significant bits of this digit are always zero, these bits are used to transfer the overload (MSB) and the display enable (MSB-1) information. A one-shot is used to stabilize the overload flag for sampling.

Selection of the system clock frequency and dividers was made so as to produce compatible binary and BCD counter frequencies. Over a complete commutation interval of 1/300 second, the 4-bit binary input to register R will increment through 2400/300 × 2 = 16 counts. Each of these counts then corresponds to 1/16th of a revolution on the LED circular display. Over the same time interval, the clock input to the BCD counters generates 108026.3736/300 = 360.0879 counts, or approximately one count per degree. Although the error is very small (less than 0.1 degree), it will accumulate rapidly unless the BCD counter is periodically synchronized back to the binary counter. The circuit consisting of flip-flop A and the surrounding gates is used to reset the three BCD counters every complete cycle (as defined by the binary counter) so that the BCD and binary counts remain synchronized.

At a rate of 2.34375 times per second (each 426.66... millisecond), data is transferred from tri-state registers O-R to latching registers S-V. Timing for the data transfer is obtained from the 12-bit counter, F, and the sequence is as follows for the case where a serial interface is not used. At the beginning of each transfer cycle (output of F all zeros), the input to registers O-R is disabled using the DID2 control inputs. These inputs remain disabled during the first quarter of the transfer cycle (106.66... milliseconds). During this same quarter cycle, the 1-of-4 decoder, Y, places the tri-state output of registers O-R sequentially onto the bus using their DOD2 control inputs. The order of selection is Q (overload/blanking/hundreds), P (tens), O (units), and R (binary). Each register is connected to the bus for 26.66... milliseconds. While a tri-state register is connected to the bus, a corresponding display register (S-V) is strobed by a short pulse generated by one-shot K-L and steered to the correct display register via a second 1-of-4 selector (Z). The data transferred to the display registers is held until the next update (426.66... milliseconds later). Consequently, the display appears stable, but is still reasonably responsive to changes in the bearing data. Also, the data displayed is consistent (i.e., the binary and BCD data displayed are sampled simultaneously even though they

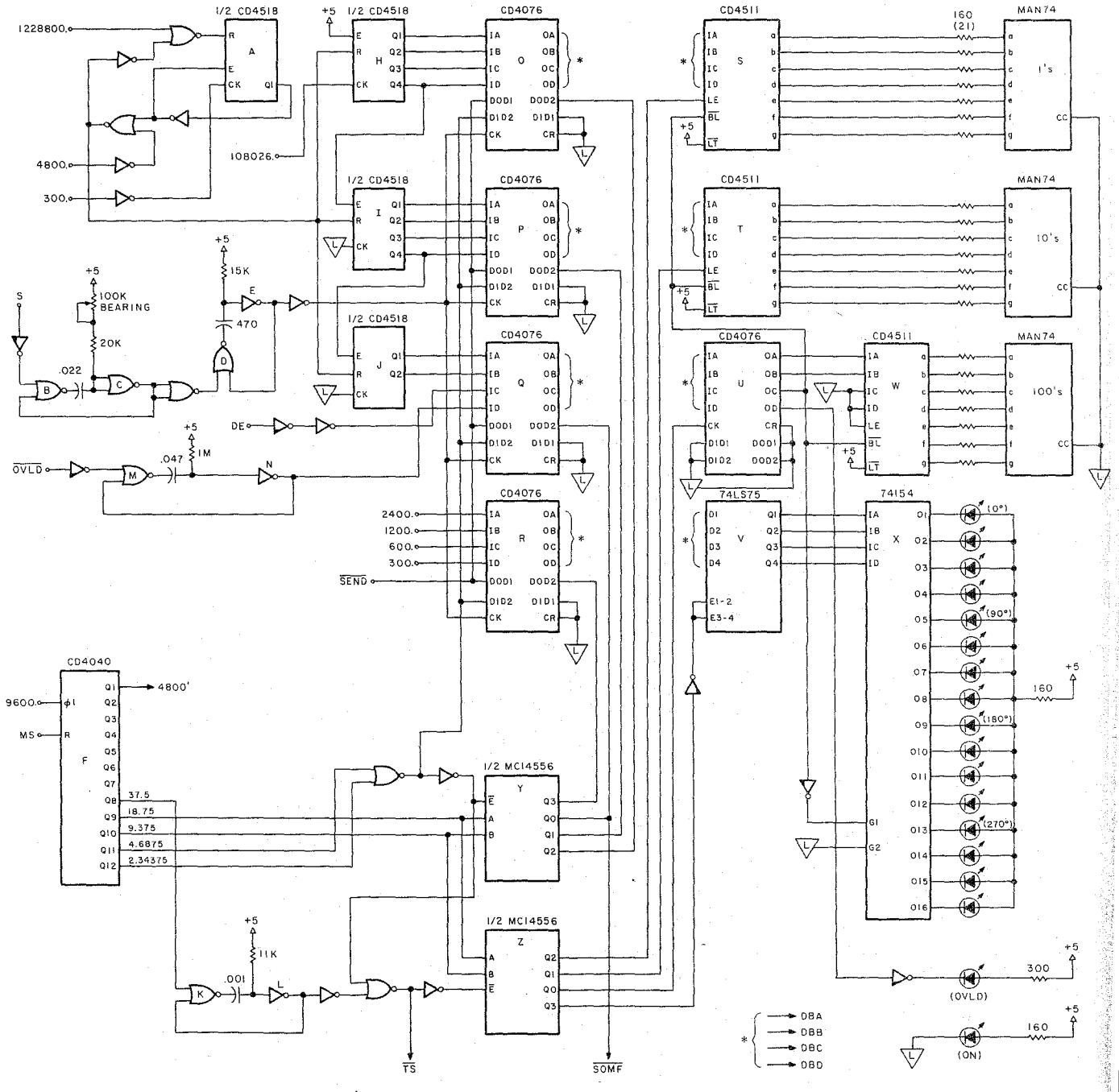

*Fig. 15. Schematic of the circuit used to provide circular LED display and a three-digit decimal display. A data bus technique is employed which is compatible with the optional serial interface. Notes: Connect 4-bit data bus *. All LEDs are MIL32 R. Digital logic power is Vdd = Vcc = +5, Vss = GND = ⏚. All NOR gates are 1/4 CD4001. All inverters are 1/6 CD4069 except ▷○ are 1/6 74C903. Schematic is drawn for operation with serial interface. For no serial interface, add jumpers SEND to ⏚, MS to ⏚.*

are transferred sequentially).

Registers S and T are CD4511 BCD-to-7-segment latching drivers which drive the units and tens displays directly. Latch U is a holding register which provides the 2 bits of hundreds data to the third CD4511 driver (W). The blanking information and overload data are also available from outputs C and D of latch U. Quad latch V provides the binary LED data to the 1-of-16 selector X.

Serial Interface

An optional serial interface is shown in Fig. 16 which permits remote transmission or reception of the displayed data using standard 300 baud audio frequency shift tones. This data rate and the FSK tones used are compatible with data recording and playback using an inexpensive tape recorder so that this interface may also be used whenever unattended operation is desired.

The universal asynchronous receiver transmitter (UART), A, is shown programmed for five data bits, no parity, and 1-1/2 stop bits per character. The first four data bits of each character are simply the four data bus bits transferred to the display registers S-V in Fig. 15. The fifth bit is used to signal the first character of the four-character message; a zero represents the first character (overload/blanking/hundreds).

When locally received data is to be displayed, the UART operates in its transmit mode. The data transfer across the data bus operates exactly as explained above, and the data bus is strobed into the UART transmit buffer whenever any of the display registers is clocked. Thus, a four-character word of data is sent every 426.66... milliseconds. At 300 baud, it requires (5 + 1-1/2)/300 seconds or 21.66... milliseconds to send each character. Since data is taken from the bus each 26.66... milliseconds, this creates a gap of 5 milliseconds between consecutive characters.

When display of remote data is selected, the timing changes somewhat. All of the tri-state registers are removed from the data bus using their DOD1 control inputs, and the UART tri-state received data output is connected to the bus ($\overline{RDE}$ = 0). When a first character has been received (bit 5 = 0 and UART data available), a pulse is generated at MS which resets 12-bit counter F in Fig. 15. Data transfer into the display registers then proceeds as usual except that the UART supplies the data. The first data character is clocked into display register U at 13.333... milliseconds following data reception. Therefore, a large skew can be tolerated between local and remote clocks without affecting system operation.

In the local data display mode, digital data at 300 baud from the UART serial output is used to select which of two clock frequencies, 9600 or 19200, is applied to the 4-bit Johnson counter, E. The counter outputs are applied through summing resistors to inverter F configured to work as an operational amplifier. The weighting of the three summing resistors is chosen such that the filtered output of F approximates a sine wave of frequency

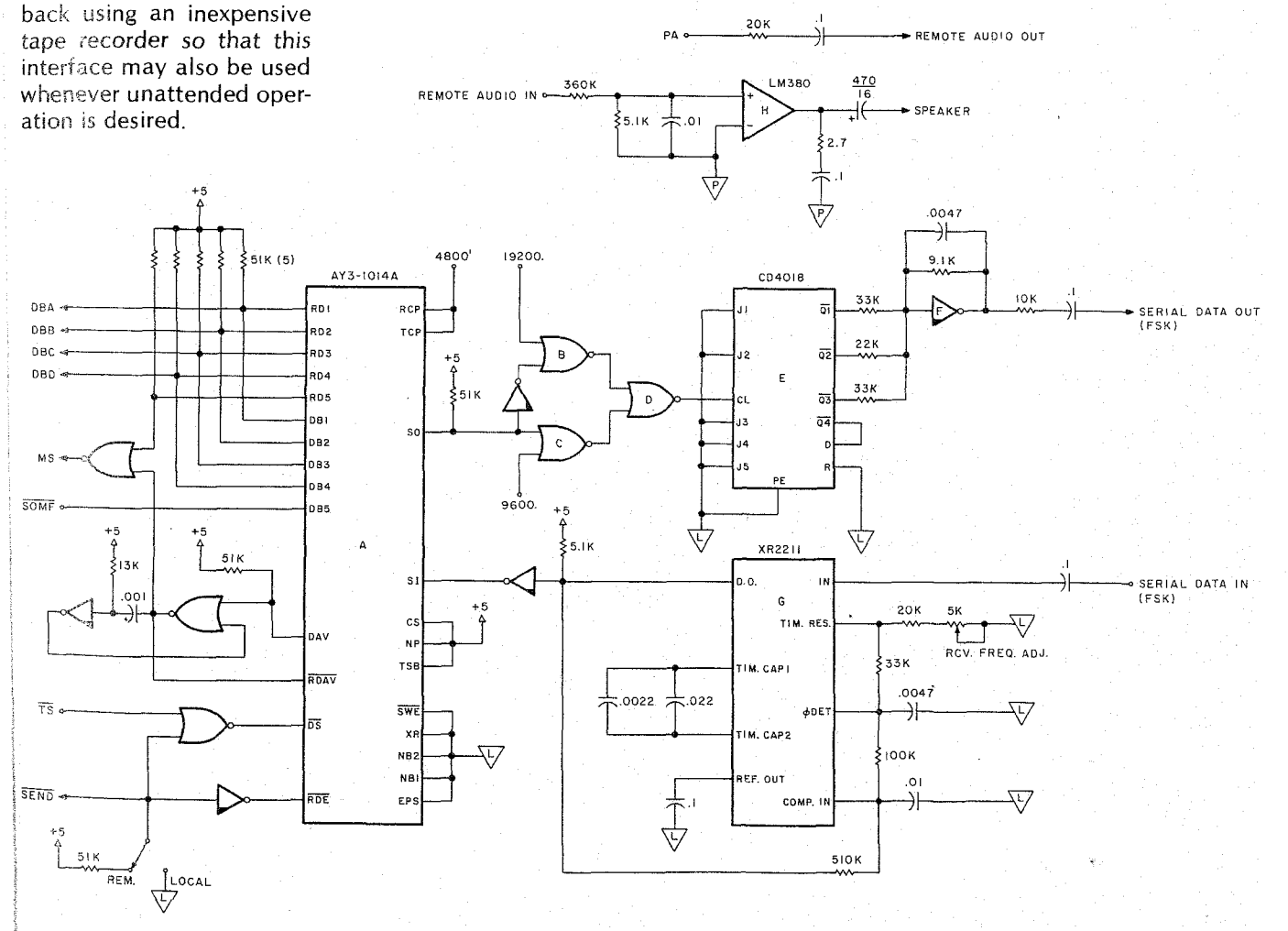

Fig. 16. Optional serial interface circuit schematic. Notes: NOR gates are 1/4 CD4001. Inverters are 1/6 74C903. Digital logic power is Vcc = Vdd = +5, Vss = GND = ⏚. Amplifier H power is +13 switched (sw); ground is Ⓟ.

1200 Hz when the UART output is "0" or 2400 Hz when the UART output is a "1". Sine-wave distortion is below 5% with this arrangement, and the FSK frequencies are as accurate as the system clock (which is crystal controlled).

When the system is in the remote data display mode, FSK input is demodulated in the XR2211 decoder, G. The component values shown are optimized for 300-baud, 1200/2400-Hz operation using the procedure given in EXAR's specification sheet for the XR2211.

The audio circuitry shown at the top of Fig. 16 is included as a convenience when using the system with a two-channel tape recorder. FSK data can be placed on one channel, and the received audio out of preamplifier A in Fig. 13 can be coupled through the RC circuit shown to the second channel for simultaneous recording. On playback, this audio is amplified by the LM380 (amplifier H) to drive a loudspeaker so that bearing data can be easily correlated with the received signal.

Power Supply and Clock

The entire system is designed to operate from a single unregulated supply voltage between 11.5 and 14.5 V dc negative ground for mobile operation. Total input current is approximately one Ampere with the display enabled. Fig. 17 shows the power supply and clock circuits.

Gates A and B are connected for linear operation and form a crystal-controlled oscillator. The 74LS197 is used to divide the 9.8304-MHz clock frequency by 8 to generate 1.2288 MHz for the antenna control waveform generator and binary display. Two 74LS193 counters are connected to divide the clock frequency by 91 to generate 108026 Hz for the BCD display. Gates F and G and the 74LS74 flip-flop are used to load a count of 256 − 91 = 165 into the two 4-bit counters. If the BCD display is not used, ICs D, E, and H may be omitted.

A 7805K regulator provides +5 V dc for the digital logic, operational amplifiers, and the displays. The 7808 regulator provides + 8 V dc for the MOSFETs used in the rf summer.

Negative voltage is generated by a switching inverter/voltage doubler circuit that produces approximately −8 V dc at the input to a 7906 regulator. The −6 V dc is used as the negative analog supply voltage.

Operational amplifier K generates the +2.0 V dc reference used for D/A conversion and threshold comparison.

Electronics Construction

If you wish to build the electronics from scratch, your best bet is to use wire-wrap sockets for all of the DIP integrated circuits and the discrete components (resistors, diodes, and small capacitors). Individual wire-wrap pins may be used for the larger components such as the electrolytic capacitors. All circuitry except the rf summer may be constructed on open perforated board with 0.1" spacing to accept the wire-wrap sockets. Be sure to bypass the +5 V dc using .047- or .1-uF disc ceramic capacitors near each of the TTL ICs and the CD4511s. Mount the 7805K regulator on a good heat sink. Be sure to use 5% resistors and either mylar or dipped mica capacitors for all of the audio filtering and digital one-shot circuits.

The rf summer circuit must be mounted in a shielded enclosure using construction practices consistent with the frequencies involved. Phono jacks work well for the antenna and

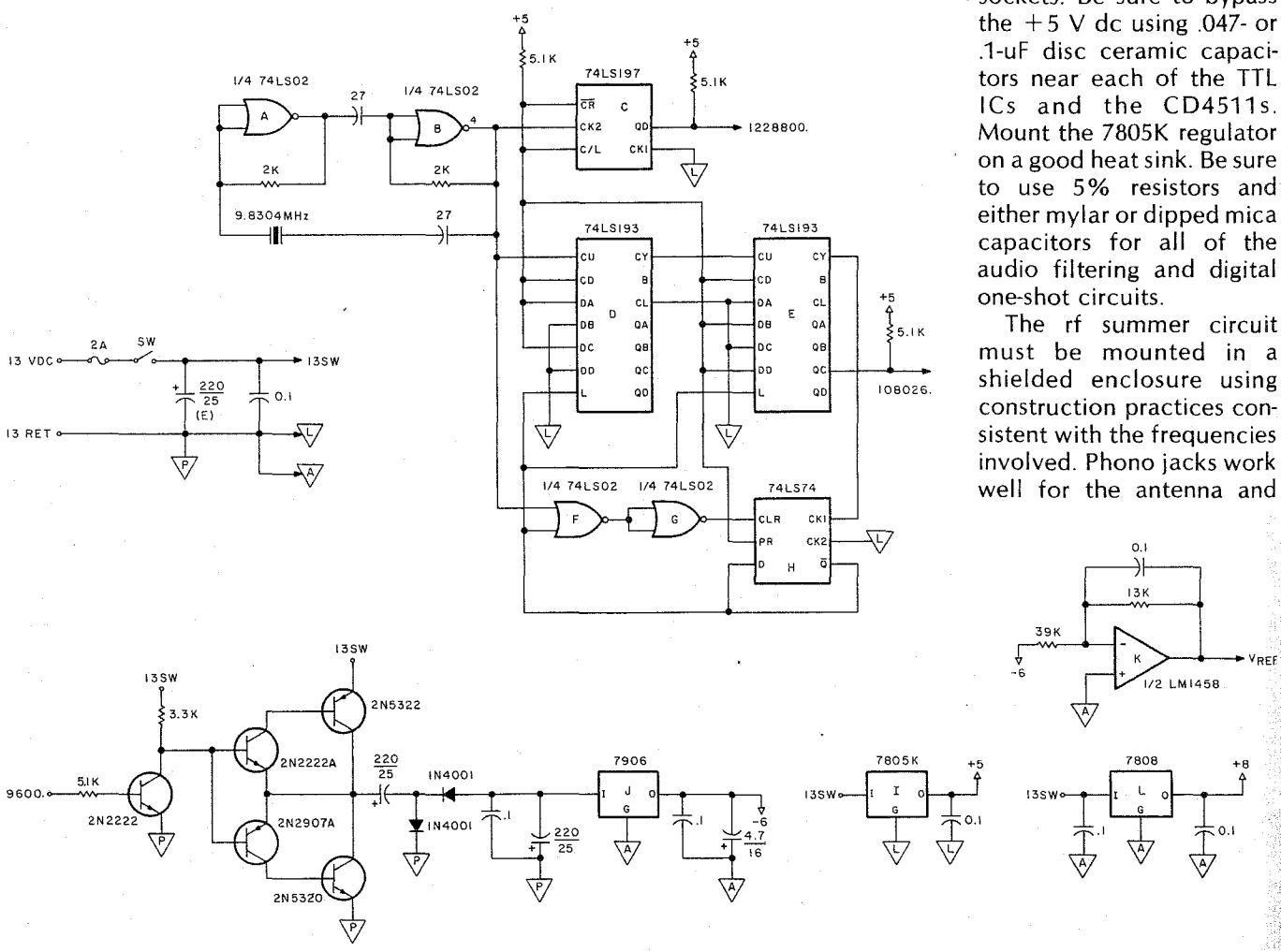

Fig. 17. Schematic of the power supply and clock circuitry. Notes: Power to LM1458 is +5 and −6 V dc. Logic power is Vcc = +5, GND = L.

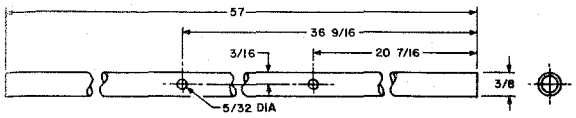

Fig. 18. Construction detail of the long radial. Two are required.

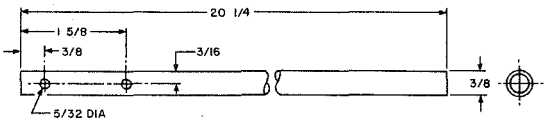

Fig. 19. Construction detail of the short radial. Four are required.

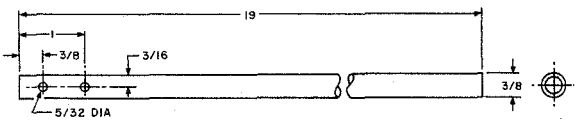

Fig. 20. Vertical element dimensions. Four are required.

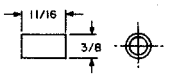

Fig. 21. Suction cup spacer. Four of these are required for mounting the antenna on a car roof.

receiver connectors. Keep all leads short and arrange the parts symmetrically.

A professionally designed unit utilizing double-sided printed wiring boards with plated-through holes and an attractive enclosure is available from Doppler Systems in either kit form or fully assembled and tested. Photo A shows the interior construction of the fully expanded version of the system (digital readout and serial interface).

Antenna Construction

The antenna array must contain four identical elements located in the corners of a square array having sides less than one-half wavelength. Analysis shows, however, that the best performance can be expected with an array size between 1/16 and 5/16 wavelength. Each element must be vertically polarized and nondirectional in the horizontal plane. Antenna impedance and matching to the transmission lines is not especially important; however, each of the four lines must be of the same electrical length. For this reason, and to prevent excessive signal loss, the antenna should not be located too far from the electronics.

Element length may be increased to provide greater capture area and may be either balanced or unbalanced using a ground plane composed of radials. Mechanical stability is important, however, especially in a mobile application.

A good basic design suitable for either fixed or mobile use is given below. Elements are approximately 1/4 wavelength long and are spaced 1/4 wavelength apart at 2 meters. Radials extend an additional 1/4 wavelength beyond the elements, giving the antenna compact and sturdy characteristics. All material should be available from local suppliers. Alternatively, specific items may be ordered from Doppler Systems.

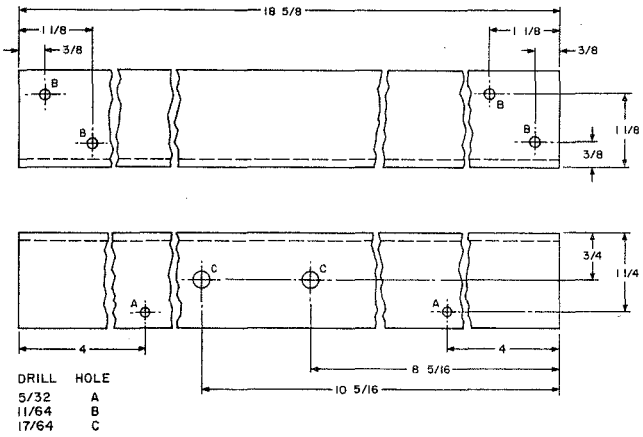

Fig. 22. Center support detail. Only one is required.

Aluminum Stock

(1)—6' × 1-1/2" × 1-1/2" × 1/8" angle
(2)—12' × 3/8" o.d. × .035"-wall tubing

Teflon

(1)—1' × 1-1/2" × 1/8" rectangular bar

Hardware

(16)—6-32 × 1/2" round head machine screws
(16)—6-32 × 3/4" round head machine screws
(4)—6-32 × 1" round head machine screws
(24)—No. 6 flat washers
(32)—No. 6 split-type lockwashers
(40)—6-32 hex nuts
(8)—No. 6 locking-type solder lugs
(4)—8-32 × 1/2" round head machine screws
(4)—No. 8 split-type lockwashers.
(4)—8-32 hex nuts
*(4)—1/4-20 × 2" eye bolts
*(8)—1/4-20 hex nuts
*(8)—1/4" split-type lockwashers
*(4)—1/4-20 × 1-1/2" bolts
*(4)—1/4" flat washers
*(4)—1/4-20 insert suction cups
*(4)—adjustable straps with gutter clips
**(1)—5/16 × 2" center-to-center × 3" long U-bolt
**(2)—5/16 split-type lockwashers
**(2)—5/16 hex nuts

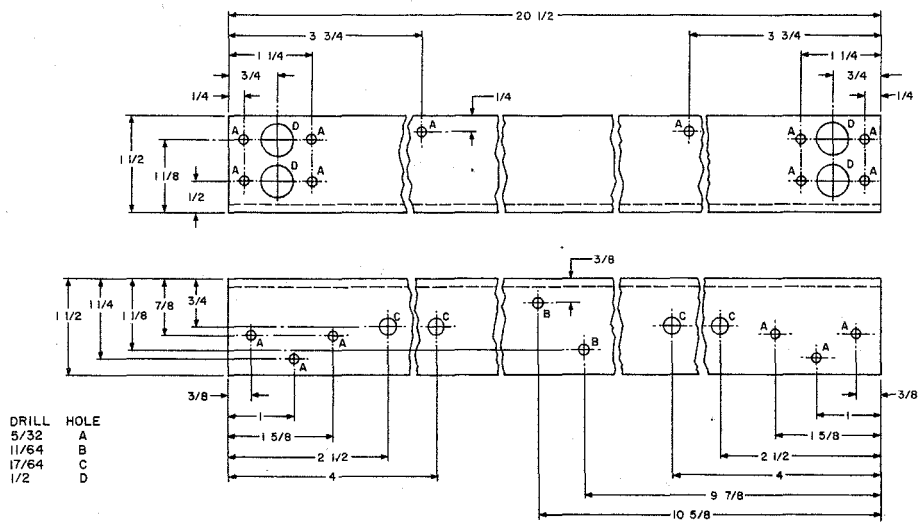

Fig. 23. Side arm construction detail. Two are required.

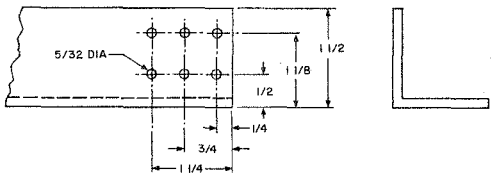

Fig. 24. Drill guide dimensions. Make this tool from stock left over from the center support and side arms.

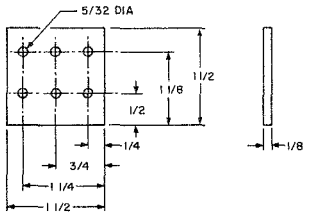

Fig. 25. Teflon insulator construction. Use the drill guide and a block of wood when drilling this material.

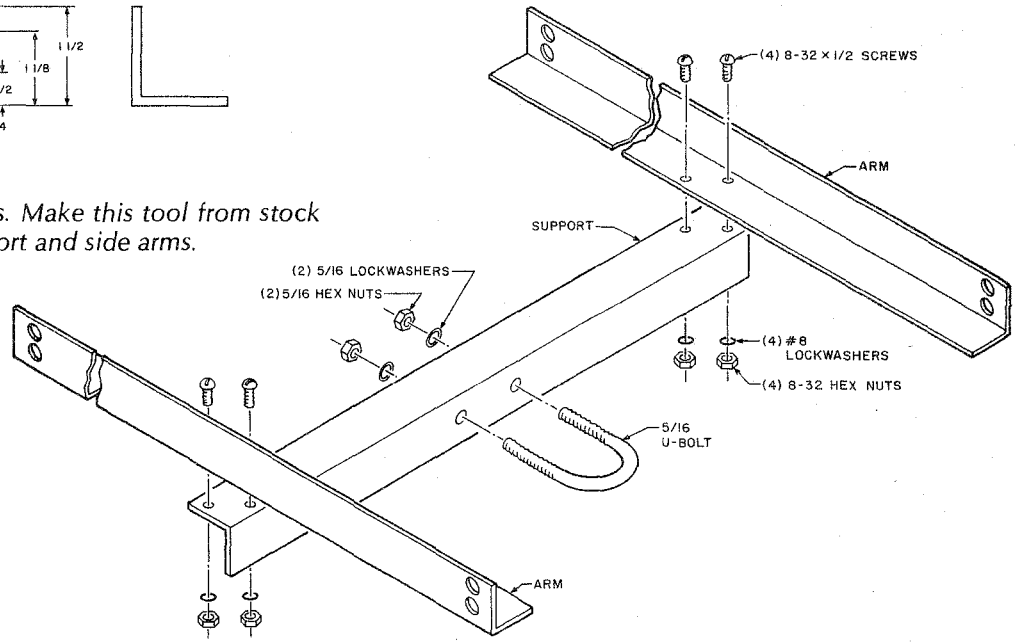

Fig. 26. Assembly of center support and side arms. The U-bolt is required only for mast mounting.

Electrical

RG-174/U coax cable (length depends on installation)
(4)—phono plugs (shielded type)
*Required for mobile mounting.
**Required for mast mounting.

Cut two pieces 20-1/2" long and one piece 18-5/8" long from the aluminum angle. Save the remaining short length for use as a drill template with the teflon. Be sure to file all ends smooth after cutting.

From each of the 12-foot pieces of tubing, cut one piece 57" long, two pieces 20-1/4" long, and two pieces 19" long. If you are making the antenna for mobile mounting, cut four additional pieces 11/16" long from the remaining short length of tubing. File all ends smooth after cutting.

Mark and drill all of the holes shown in Figs. 18 through 24. Use a countersink to deburr all of the holes after drilling.

Cut the teflon into four pieces 1-1/2" long as shown in Fig. 25. Clamp the four teflon pieces together between a piece of wood and the end of the drill guide. Drill the six 5/32"-diameter holes through all four pieces.

Prepare four lengths of coax cable by soldering No. 6 solder lugs to both the inner conductor and the shield at one end, and a phono plug at the other. Be sure that the four pieces are cut to the same length.

Assemble the two arms to the support bracket using the 8-32 hardware as shown in Fig. 26. Use a square to align the arms perpendicular to the support before tightening the screws.

At each end of the two arms, assemble a vertical element using the 6-32 hardware and teflon insulator as shown in Fig. 27. Check that the element is perpendicular to the arm and that the element mounting hardware does not touch the aluminum arm. Tighten the screws sufficiently to compress the lockwashers, but do not overtighten so as to crush the tubing or the teflon insulator. Connect the coax cable and tie it as shown as a strain relief.

Attach the short and long radials to the ends of each arm using the 6-32 hardware shown in Fig.28. If the antenna will be used on a car, also mount the suction cups and eye bolts as shown. Align the "eyes" so that they face outward from the suction cups. Photo B shows a typical installation.

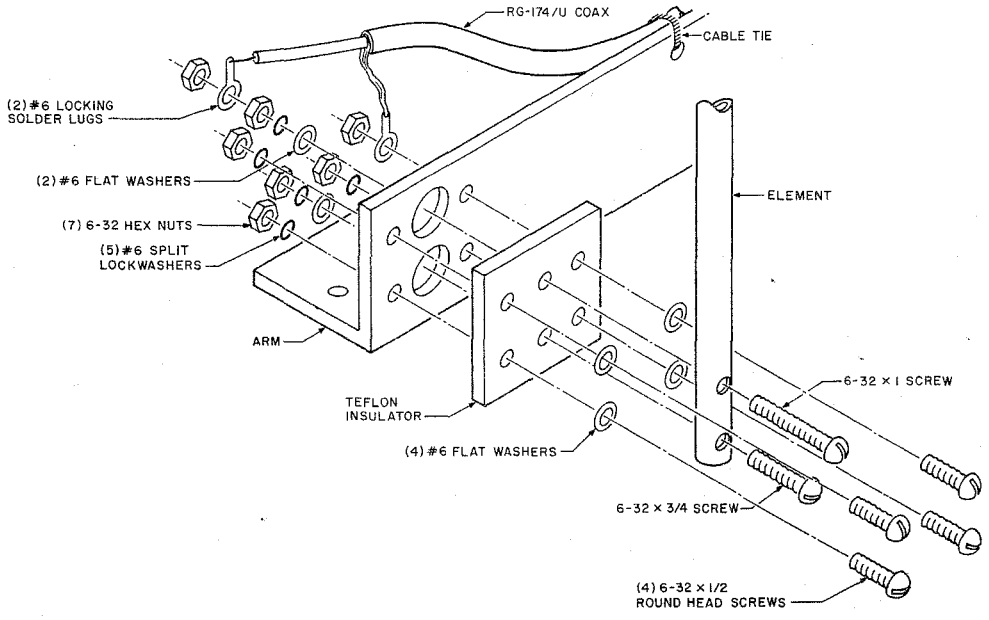

Fig. 27. Vertical element installation on the antenna side arms.

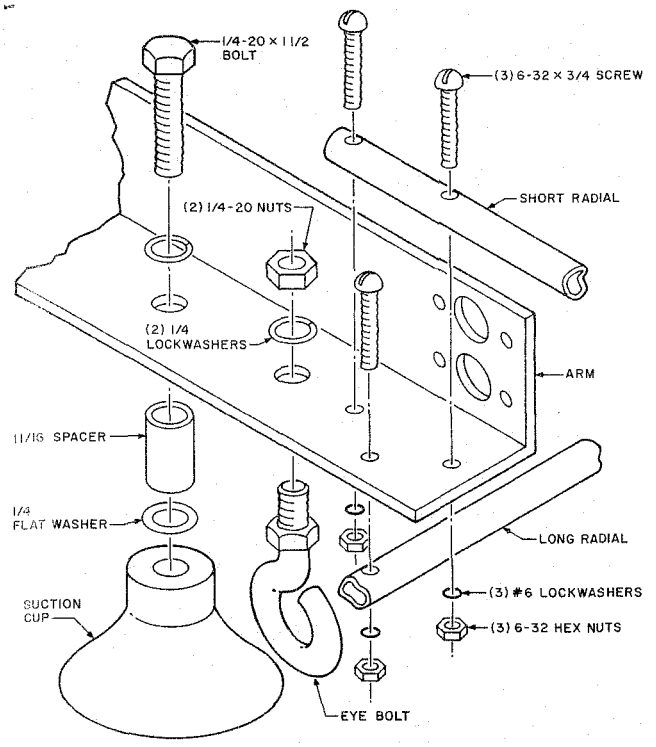

Fig. 28. Radial element assembly. The eye bolt and suction cups are required only for car mounting.

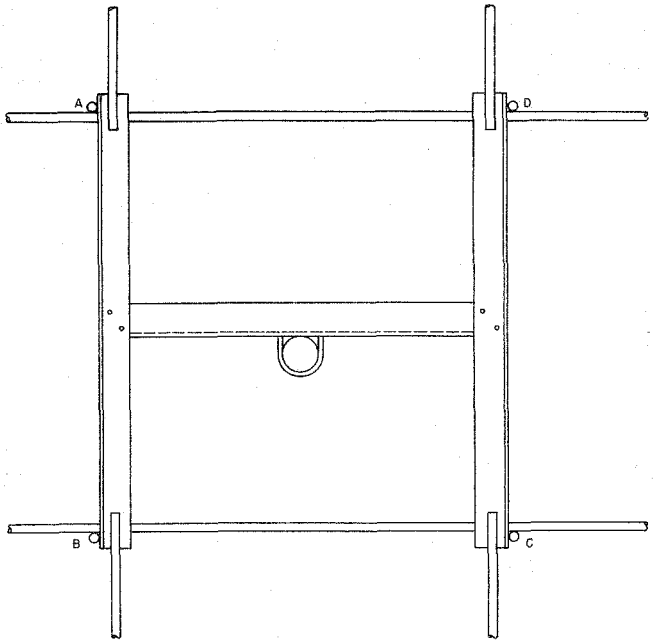

Fig. 29. Antenna top view showing marking of phono plugs required for proper calibration.

Mark the phono jack ends of the coax cable "A", "B", "C", and "D" according to Fig. 29. Mark antenna "A" also for ease in aligning the system later.

Installation and Adjustment

Primary power requirements for the electronics is 11.5 to 13.5 V dc negative ground at 1 Ampere maximum. Ordinary 12-V dc automobile battery power may be used, or, for fixed operation, an inexpensive 12.6-V dc power supply may be used, such as Radio Shack Model 22-127.

System interconnection without the serial interface is particularly simple as indicated in Fig. 30. While the external speaker connection can be used, you will probably find a more convenient connection to be the high and low ends of the receiver's volume control. This will enable the listening level of the receiver to be adjusted without affecting the audio input level to the direction finder.

The serial interface can be used in several ways as indicated in Figs. 31 and 32. Bearing data and receiver audio may be recorded simultaneously as shown in Fig. 31. Virtually any audio tape recorder is adequate for this application because of the low baud rate and wide FSK shift used for serial data transmission. A stereo system is recommended so that the normal receiver audio (voice) information may be recorded with the bearing data.

Two systems may be connected as shown in Fig. 32 for remote data display. A switch could be installed at the central site to enable a single monitor point to display the bearing data received at two or more remote sites for triangulation. The possibilities for more complex system interconnects using digital processing for automatic triangulation and logging are exciting.

Calibration adjustments are very simple and should not be required after initial setup unless the antenna orientation is changed or a different receiver is used. Allow the receiver and direction finder to warm up before making final calibration adjustments, however.

After setting the receiver's volume control, the direction-finder gain adjustment is made. Increase the gain until the overload LED flashes on voice peaks. (If this adjustment is very low, the display will remain blanked.) Setting is not critical, but the overload LED should blink with a duty cycle between about 10 and 50 percent during normal speech.

The direction-finder bearing control should then be adjusted so that the correct bearing is displayed for a known transmitted signal. Do not use a nearby handie-talkie for this calibration as local reflections are sure to result in an error. A repeater station which is within the line of sight of the antenna makes the best calibration source. Changing channels will have very little effect on system calibration, so any convenient station within the band may be used. The display should be

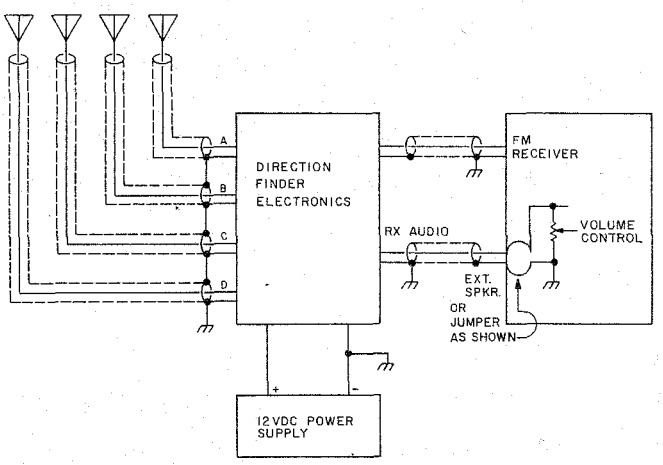

Fig. 30. Basic system connection to antenna, power source, and FM receiver. If a transceiver is used, be sure to disable the transmitter to prevent inadvertent transmission into the RDF electronics.

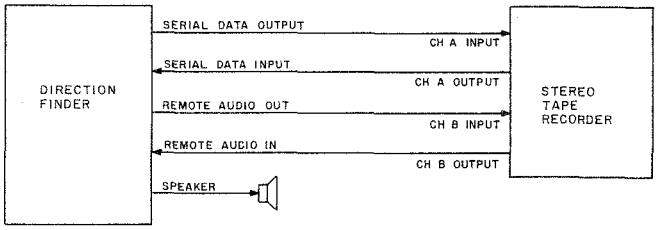

Fig. 31. Serial interface connection for tape recording and playback.

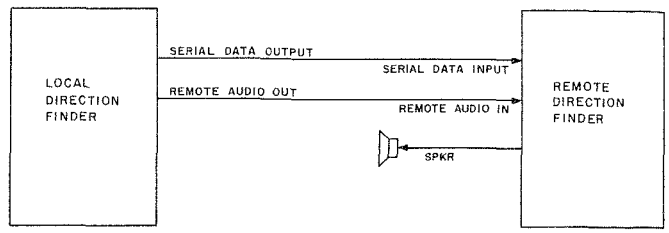

Fig. 32. Use of serial interface for remote display of bearing data.

calibrated to display bearing relative to magnetic North in a fixed station setup and should correspond to straight ahead in a mobile application. The calibration range of the bearing control is approximately 90 degrees. If the system needs further correction, either rotate the antenna physically or switch the antenna inputs to the electronics. Be sure not to reverse the order of antenna rotation, however. The acceptable combinations for inputs A, B, C, and D are: Ant. A, Ant. B, Ant. C, Ant. D; or Ant. D, Ant. A, Ant. B, Ant. C; or Ant. C, Ant. D, Ant. A, Ant. B; or Ant. B, Ant. C, Ant. D, Ant. A. See Fig. 8 for definition of antenna inputs to rf summer and Fig. 29 for the definition of antenna elements.

If the serial interface option is to be used, the receive frequency adjustment can be made by recording a few minutes of data, then playing it back in the Remote Display Mode while making this adjustment. Note the control settings where invalid data occur, then set the control midway between these settings. If valid data is received up to one of the ends of the control adjustment, use the end point as the invalid data point. The setting of this control is not very critical.

Accuracy tests have been performed using fixed-signal sources and a fixed-receiving site to eliminate changing reflection paths. The antenna was rotated on a calibrated turnstile and errors measured between the true bearing and the displayed bearing. These were generally well within 5 degrees except when the transmitted audio was unusually loud or deep-voiced. Even in those cases, better bearing data could be obtained by mentally averaging the displayed data.

Field testing has occured over the past year using the system competitively in local transmitter hunting. The success record achieved to date has been very impressive considering the high expertise in transmitter hunting which exists in the Phoenix area. ■